Mott insulator to superfluid transition of ultracold bosons in an optical lattice near a Feshbach resonance

K. Sengupta[1] and N. Dupuis[2]

[1] *Department of Physics, Yale university, New Haven, CT-06520-8120*
[2] *Laboratoire de Physique des Solides, CNRS UMR 8502, Université Paris-Sud, 91405 Orsay, France*

Abstract. – We study the phase diagram of ultracold bosons in an optical lattice near a Feshbach resonance. Depending on the boson density, the strength of the optical lattice potential and the detuning from resonance, the ground state can be a Mott insulator, a superfluid phase with both an atomic and a molecular condensate, or a superfluid phase with only a molecular condensate. Mott insulator to superfluid transitions can be induced either by decreasing the strength of the optical lattice potential or by varying the detuning from the Feshbach resonance. Quite generally, we find that for a commensurate density the ground-state may undergo several insulator-superfluid or superfluid-insulator transitions as the magnetic field is varied through the resonance.

Recent experiments on ultracold trapped atomic gases have opened a new window onto the phases of quantum matter [1]. A gas of bosonic atoms in an optical or magnetic trap has been reversibly tuned between superfluid (SF) and insulating ground states by varying the strength of a periodic potential produced by standing optical waves. This transition has been explained on the basis of the Bose-Hubbard model with on-site repulsive interactions and hopping between nearest neighboring sites of the lattice [2]. As long as the atom-atom interactions are small compared to the hopping amplitude, the ground state remains superfluid. In the opposite limit of a strong lattice potential, the interaction energy dominates and the ground state is a Mott insulator (MI) when the density is commensurate, with an integer number of atoms localized at each lattice site. Another aspect of trapped bosonic atoms that has been studied extensively in recent years (without the optical lattice) is the dramatic increase in the effective atom-atom interaction due to the presence of a Feshbach resonance [3,4]. Near the resonance, which can be experimentally realized by tuning an external magnetic field, the atoms can resonantly collide to form molecular bound states. Remarkable phenomena associated with a Feshbach resonance, including coherent atom-molecule oscillations and collapse of the Bose-Einstein condensate, have been experimentally observed [4].

In this Letter, we study a Bose gas in the presence of an optical lattice near a Feshbach resonance. Starting from an effective Bose-Hubbard Hamiltonian, we first obtain the various

Mott insulating states that are stable in the limit of a strong optical lattice. We then study the stability of these states by deriving an effective Landau-Ginzburg theory for the MI-SF transition. Depending on the boson density, the strength of the optical lattice potential and the detuning from resonance, the ground state can be a MI, a SF phase with both an atomic and a molecular condensate, or a SF phase with only a molecular condensate. MI-SF transitions can be induced either by decreasing the strength of the optical lattice potential or by varying the detuning from the Feshbach resonance. For odd commensurate densities, Mott phases are found to be always unstable to superfluidity on the molecular side of the Feshbach resonance. For even commensurate densities, Mott phases can be stable on both sides of the resonance and may undergo several MI-SF or SF-MI transitions as the magnetic field is varied through the resonance.

Bosons in an optical lattice near a Feshbach resonance can be described by the generalized Bose-Hubbard Hamiltonian

$$
\begin{aligned}
H \; = \; & \sum_{\sigma=a,m} \left[-t_\sigma \sum_{\langle \mathbf{r},\mathbf{r}'\rangle} (\psi_\sigma^\dagger(\mathbf{r})\psi_\sigma(\mathbf{r}') + \text{h.c.}) - \mu_\sigma \sum_{\mathbf{r}} \psi_\sigma^\dagger(\mathbf{r})\psi_\sigma(\mathbf{r}) \right. \\
& \left. + \frac{U_\sigma}{2} \sum_{\mathbf{r}} \psi_\sigma^\dagger(\mathbf{r})\psi_\sigma^\dagger(\mathbf{r})\psi_\sigma(\mathbf{r})\psi_\sigma(\mathbf{r}) \right] \\
& + U_{am} \sum_{\mathbf{r}} \psi_a^\dagger(\mathbf{r})\psi_m^\dagger(\mathbf{r})\psi_m(\mathbf{r})\psi_a(\mathbf{r}) - \alpha \sum_{\mathbf{r}} (\psi_m^\dagger(\mathbf{r})\psi_a(\mathbf{r})\psi_a(\mathbf{r}) + \text{h.c.}). \quad (1)
\end{aligned}
$$

$\psi_\sigma, \psi_\sigma^\dagger$ are bosonic operators for atoms ($\sigma = a$) and molecules ($\sigma = m$). The discrete variable $\mathbf{r}$ labels the different sites (i.e. minima) of the optical lattice. $\langle \mathbf{r},\mathbf{r}'\rangle$ denotes a sum over nearest sites. The optical lattice is assumed to be bipartite with coordination number z. t_σ is the intersite hopping amplitude, and U_σ the amplitude of the atom-atom ($\sigma = a$) or molecule-molecule ($\sigma = m$) interaction. U_{am} gives the amplitude of atom-molecule interactions. $\mu_a = \mu$ and $\mu_m = 2\mu - \nu$ are the chemical potential for atoms and molecules. The chemical potential μ fixes the total number of atoms (free or bound into molecules). ν is related to the energy of a molecular bound state and is a function of the applied magnetic field. A negative detuning from resonance ($\nu < 0$) favors the formation of molecules. The last term in Eq. (1) describes the atom-molecule conversion and the parameter α depends on the resonance width [3, 4]. The Hamiltonian (1) can be derived from a microscopic model starting from the bare atom-molecule Hamiltonian in the presence of the optical lattice [4] and expanding the operators ψ_a, ψ_m on the lowest-band Wannier states [5]. We shall not attempt to calculate the explicit values of $U_\sigma, t_\sigma, U_{am}$ and α from the microscopic Hamiltonian, but rather treat them as free parameters. We take $U_a = U_m = 1$ and $\alpha = 0.5$, and vary U_{am} and $t_a = t_m$ since the qualitative aspects of the phase diagram do not depend on the precise values of α, U_a/U_m and t_m/t_a [6]. We also neglect the trap potential, which is not expected to change qualitatively the main conclusions of our work.

Let us first discuss the phase diagram in the "local" (i.e. single-site) limit where $t_a = t_m = 0$. For an integer number n_0 of particles per site, the Hilbert space is spanned by the states $|n_a, n_m\rangle = (n_a! n_m!)^{-1/2}(\psi_a^\dagger)^{n_a}(\psi_m^\dagger)^{n_m}|\text{vac}\rangle$ where the number of atoms (n_a) and molecules (n_m) satisfy $n_a + 2n_m = n_0$. $|\text{vac}\rangle$ denotes the vacuum of particles. In this basis, the Hamiltonian $H^{(n_0)}$ is a real symmetric matrix, defined by

$$
\begin{aligned}
H^{(n_0)}_{n_m,n_m} \; &= \; -\mu n_0 + \nu n_m + \frac{U_a}{2} n_a(n_a - 1) + \frac{U_m}{2} n_m(n_m - 1) + U_{am} n_a n_m, \\
H^{(n_0)}_{n_m-1,n_m} \; &= \; -\alpha[(n_a + 2)(n_a + 1)n_m]^{1/2}, \quad\quad\quad\quad\quad\quad\quad\quad\quad\quad\quad\quad\quad\quad (2)
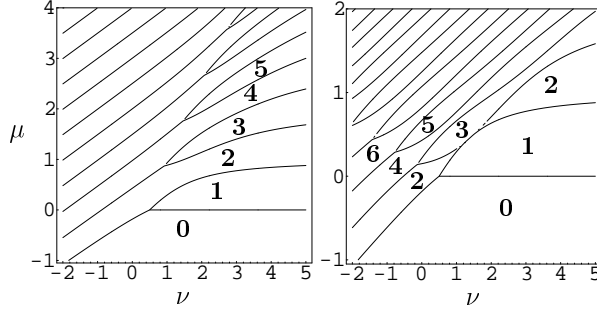\end{aligned}
$$

Fig. 1 – Phase diagram in the local limit ($t_a = t_m = 0$) vs chemical potential μ and detuning ν from the Feshbach resonance. $\alpha = 0.5$, $U_a = U_m = 1$. $U_{am} = 1$ (left), $U_{am} = 0.25$ (right). Each phase is labeled by the number n_0 of atoms (free or bound into molecules) per site.

which can be numerically diagonalized. In the following we shall denote the eigenstates and eigenenergies by $(\phi_i^{(n_0)}, E_i^{(n_0)})$, $i = 1, \cdots, d_{n_0}$, where $d_{n_0} = n_0/2 + 1$ $((n_0 + 1)/2)$ for n_0 even (odd).

The phase diagram in the local limit as a function of the chemical potential μ and the detuning ν is shown in Fig. 1 for $U_{am} = 1$ and $U_{am} = 0.25$. Each phase is labeled by the total number $n_0 = n_a + 2n_m$ of bosons per site where n_a and n_m are the mean number of atoms and molecules. First let us consider the Mott states for large detuning $|\nu|/\alpha \gg 1$. For even n_0, the Mott states are stable on both sides of the resonance: for $\nu > 0$, there are $n_a = n_0$ atoms per site whereas for $\nu < 0$ there are $n_m = n_0/2$ molecules per site. For n_0 odd, the MI's are stable only for $\nu > 0$. For $\nu < 0$, the ground state for odd n_0 is a superposition of two Mott phases with $(n_0 - 1)/2$ and $(n_0 + 1)/2$ molecules per site and hence unstable to superfluidity for any finite t_a, t_m. The phase diagram for small detuning ($|\nu|/\alpha < 1$), on the other hand, depends crucially on U_{am}. In contrast to the case $U_{am} \geq 1$, for $U_{am} \ll 1$, the Mott phases with odd n_0 can occur even when $\nu < 0$ as seen in Fig. 1.

In order to study the instability of the Mott phases towards superfluidity in the presence of finite intersite hopping, we perform an expansion about the local limit. Our approach is a generalization of mean-field theories previously used for the Bose-Hubbard model [7]. We write the partition function Z as a functional integral over complex bosonic fields ψ_a, ψ_m with the action $S[\psi_a, \psi_m] = \int_0^\beta d\tau \{\sum_{\mathbf{r},\sigma} \psi_\sigma^*(\mathbf{r}) \partial_\tau \psi_\sigma(\mathbf{r}) + H[\psi]\}$ (τ is an imaginary time and $\beta = 1/T$ the inverse temperature). Introducing an auxiliary field ϕ_σ to decouple the intersite hopping term by means of a Hubbard-Stratonovich transformation, we obtain

$$
\begin{aligned}
Z &= \int \mathcal{D}[\psi, \phi] e^{-(\phi|t^{-1}\phi)+((\phi|\psi)+\text{c.c.})-S_0[\psi]} \\
&= Z_0 \int \mathcal{D}[\phi] e^{-(\phi|t^{-1}\phi)} \left\langle e^{(\phi|\psi)+\text{c.c.}} \right\rangle_0 \\
&= Z_0 \int \mathcal{D}[\phi] e^{-(\phi|t^{-1}\phi)+W[\phi]},
\end{aligned}
\tag{3}
$$

where we use the shorthand notation $(\phi|\psi) = \int_0^\beta d\tau \sum_{\mathbf{r},\sigma} \phi_\sigma^*(\mathbf{r}) \psi_\sigma(\mathbf{r})$, etc. t^{-1} denotes the inverse of the intersite hopping matrix defined by $t^\sigma_{\mathbf{r}\mathbf{r}'} = t_\sigma$ if $\mathbf{r}, \mathbf{r}'$ are nearest neighbors and $t^\sigma_{\mathbf{r}\mathbf{r}'} = 0$ otherwise. S_0 is the action of the ψ field in the local limit ($t_a = t_m = 0$). $\langle \cdots \rangle_0$ means that the average is taken with $S_0[\psi]$. In the last line of (3), we have introduced the
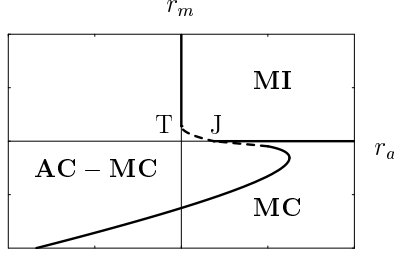
Fig. 2 – Mean-field phase diagram obtained from the free energy F [Eq. (5)]. MI: Mott insulator, AC-MC: SF phase with AC and MC, MC: SF phase with MC. The solid (dashed) lines indicate second (first) order transitions. $T = (0, \Lambda^2 (g_m/g_a)^{1/2}/[4(g_a g_m)^{1/2}+g_{am}])$ and $J = (\Lambda^2/[4(g_a g_m)^{1/2}+g_{am}], 0)$ separate second and first order MI-SF transition lines.

generating functional of connected local Green's functions [8]:

$$
\begin{aligned}
W[\phi] \;=\; & -\sum_{\sigma,1,2} \phi_\sigma^*(1) G_\sigma(1,2) \phi_\sigma(2) + \frac{1}{4}\sum_{\sigma,1,2,3,4} G_\sigma^{\mathrm{IIc}}(1,2;3,4)\phi_\sigma^*(1)\phi_\sigma^*(2)\phi_\sigma(4)\phi_\sigma(3) \\
& + \sum_{1,2,3,4} G_{am}^{\mathrm{IIc}}(1,2;3,4)\phi_a^*(1)\phi_m^*(2)\phi_m(4)\phi_a(3) \\
& + \frac{1}{2}\sum_{1,2,3}[\Lambda_{am}(1,2;3)\phi_a^*(1)\phi_a^*(2)\phi_m(3) + \mathrm{c.c.}],
\end{aligned}
\tag{4}
$$

up to quartic order in the fields. Here $i \equiv (\mathbf{r}_i, \tau_i)$ and $\sum_i \equiv \int_0^\beta d\tau_i \sum_{\mathbf{r}_i}$. $G_\sigma(1,2) = -\langle \psi_\sigma(1)\psi_\sigma^*(2)\rangle_0$, $G_\sigma^{\mathrm{IIc}}(1,2;3,4) = \langle \psi_\sigma(1)\psi_\sigma(2)\psi_\sigma^*(4)\psi_\sigma^*(3)\rangle_{0,c}$ and $G_{am}^{\mathrm{IIc}}(1,2;3,4) = \langle \psi_a(1)\psi_m(2)\psi_m^*(4)\psi_a^*(3)\rangle_{0,c}$ are single-particle and two-particle connected local Green's functions, and $\Lambda_{am}(1,2;3) = \langle \psi_a(1)\psi_a(2)\psi_m^*(3)\rangle_0$.

We determine the zero-temperature phase diagram within a mean-field approximation where ϕ_a and ϕ_m are assumed to be time and space independent. A finite value of ϕ_σ signals superfluidity since $\phi_\sigma = zt_\sigma \langle \psi_\sigma \rangle$ at the mean-field level. The free energy (per site) F is obtained to quartic order from Eqs. (3,4):

$$
F = F_0 + \sum_\sigma \left(r_\sigma \phi_\sigma^2 + \frac{g_\sigma}{2}\phi_\sigma^4 \right) + g_{am}\phi_a^2\phi_m^2 - \Lambda\phi_a^2\phi_m,
\tag{5}
$$

where, with no loss of generality, the order parameters can be chosen real. $F_0 = -T\ln Z_0$ is the free energy in the local limit. The coefficients of the free energy expansion (5) are given by $r_\sigma = (zt_\sigma)^{-1} + G_\sigma$, $g_\sigma = -G_\sigma^{\mathrm{IIc}}/2$, $g_{am} = -G_{am}^{\mathrm{IIc}}$, and $\Lambda = \Lambda_{am}$ where all the local Green's functions are evaluated in the static limit and for $T \to 0$. For instance $G_\sigma \equiv G_\sigma(i\omega = 0)$, where $G_\sigma(i\omega)$ is the Fourier transform of $G_\sigma(\tau)$ (ω is a bosonic Matsubara frequency). The mean-field phase diagram obtained from F is shown in Fig. 2 [9]. There are three different ground states: MI: $\phi_a = \phi_m = 0$, SF phase with both an atomic and a molecular condensate (AC-MC): $\phi_a, \phi_m \neq 0$, and SF phase with only a molecular condensate (MC): $\phi_a = 0, \phi_m \neq 0$. The existence of two different SF phases in a Bose-Einstein condensate near a Feshbach resonance has been recently predicted in Ref. [10] [11]. Both SF phases spontaneously break the U(1) gauge invariance, i.e. the invariance under the phase transformations $\phi_a \to \phi_a e^{i\theta}$ and $\phi_m \to \phi_m e^{2i\theta}$. The MC phase breaks only the U(1)/$\mathbb{Z}_2$ symmetry since $\phi_m \to \phi_m$ for $\theta = \pi$. The residual discrete $\mathbb{Z}_2$ symmetry is spontaneously broken at the (Ising-like) transition to the AC-MC phase which occurs near the resonance [10].
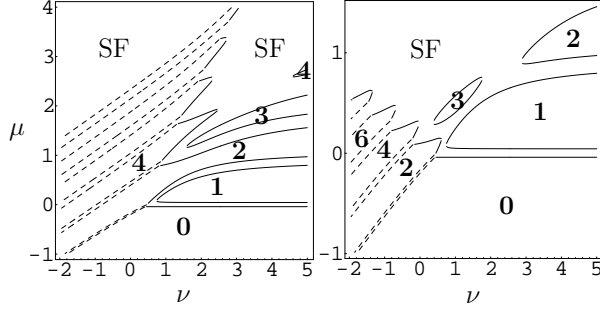
Fig. 3 – Same as Fig. 1, but for a finite intersite hopping $zt_a = zt_m = 0.04$. The MI's (labeled by the number n_0 of atoms (free or bound into molecules) per site) are surrounded by SF phases. The solid (dashed) lines indicate a transition from a MI to an AC-MC (MC) SF phase. Transition lines between AC-MC SF phases and MC SF phases are not shown.

The phase transitions are second order except near $r_a = r_m = 0$ where they become first order (Fig. 2) [12]. In the following, we neglect the possibility of first-order phase transitions so that the phase boundaries of the Mott insulating phases are determined by $r_a = 0$ or $r_m = 0$. This approximation overestimates the stability of the Mott phases, but is expected to give a correct qualitative description of the phase diagram. Since the region where first-order phase transitions occur shrinks with Λ (and therefore α), as shown in Fig. 2, this approximation should be quantitatively correct when $\alpha \ll U_a, U_m, U_{am}$.

To proceed further, we need to determine r_σ and therefore the single-particle local Green's function G_σ. Using the eigenstates $\phi_i^{(n_0)}$ of $H^{(n_0)}$, we find (for $T = 0$)

$$G_\sigma = - \sum_{i=1}^{d_{n_0-p_\sigma}} \frac{|\langle \phi_i^{(n_0-p_\sigma)}|\psi_\sigma|\phi_1^{(n_0)}\rangle|^2}{E_i^{(n_0-p_\sigma)} - E_1^{(n_0)}} + \sum_{i=1}^{d_{n_0+p_\sigma}} \frac{|\langle \phi_1^{(n_0)}|\psi_\sigma|\phi_i^{(n_0+p_\sigma)}\rangle|^2}{E_1^{(n_0)} - E_i^{(n_0+p_\sigma)}}, \tag{6}$$

where $p_a = 1$ and $p_m = 2$, and $\phi_1^{(n_0)}$ denotes the ground state of $H^{(n_0)}$. Fig. 3 shows the phase diagram in the (ν, μ) plane for $zt_a = zt_m = 0.04$. Mott phases with different n_0 are now separated by SF phases. Transitions between AC-MC and MC phases, which are beyond the scope of this Letter, are not shown. MI's with odd and even commensurate densities (to be referred to as "odd" and "even" MI's in the following) exhibit different behaviors. As $t_a = t_m$ increases, odd MI's become instable towards an AC-MC SF phase and are pushed to higher values of ν. Above the critical value $zt_a^{(c)} = U_a(2n_0 + 1 + \sqrt{n_0^2 + n_0})^{-1}$, the odd MI with n_0 atoms per site has become entirely superfluid. The behavior of even MI's is more involved. They can be stable on both sides of the Feshbach resonance, and are unstable both towards AC-MC and MC phases as ν, μ or $t_a = t_m$ are varied. The phase diagram and the disappearance of the MI's as $t_a = t_m$ increases turns out to be strongly dependent on the precise values of U_{am} and α, as well as on U_a/U_m and t_a/t_m. Quite generally, however, we find that for a commensurate density and certain values of the strength of the optical lattice the ground-state may undergo several MI-SF or SF-MI transitions as ν is varied. This phenomenon always occurs for even commensurate densities [see Fig. 3 for $n_0 = 4$ (left panel) and $n_0 = 2$ (right panel)] but is restricted to small values of U_{am} for odd commensurate densities [right panel of Fig. 3 for the $n_0 = 3$ phase].

The difference between odd and even phases is also clearly seen by considering the phase diagram at constant density. The density n is given by $n = -\partial F/\partial \mu$. In the SF phase near
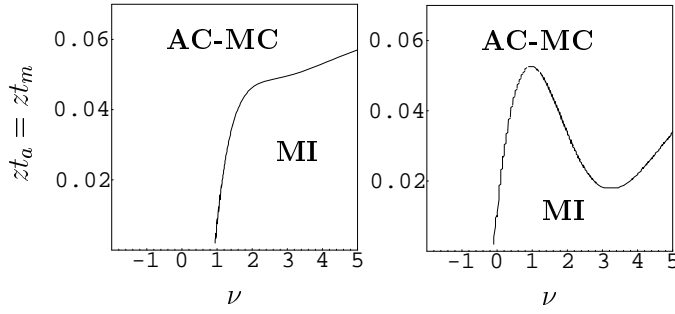
Fig. 4 – Phase diagram for $n = 3$ *vs* intersite hopping amplitude $t_a = t_m$ and detuning ν from the Feshbach resonance. $\alpha = 0.5$ and $U_a = U_m = 1$. $U_{am} = 1$ (left), $U_{am} = 0.25$ (right).

the SF-MI transition, we obtain

$$
n = \begin{cases}
n_0 + \dfrac{r_a}{g_a - \frac{\Lambda^2}{2r_m}} \dfrac{\partial r_a}{\partial \mu} & \text{(AC} - \text{MC phase)} \\[2ex]
n_0 + \dfrac{r_m}{g_m} \dfrac{\partial r_m}{\partial \mu} & \text{(MC phase)}
\end{cases}
\tag{7}
$$

where n_0 is the density of the nearby MI. Thus at the transition points where $\partial_\mu r_\sigma = 0$, the density n remains commensurate and equal to n_0. The condition $\partial_\mu r_\sigma = 0$ implies that the boundary between the MI and the SF phases has a vertical tangent in the (ν, μ) plane (Fig. 3). The phase diagrams for $n = 3$ and $n = 2$ are shown in Figs. 4 and 5. As discussed above, we observe MI-SF and SF-MI transitions as ν is varied at constant $t_a = t_m$. For large U_{am}, the MI will be more robust for an integer mean number of atoms and molecules, whereas for small U_{am} it is more likely to become superfluid. This explains why the behavior of the $n = 2$ phase near $\nu \sim 1$ is strongly dependent on U_{am} (Fig. 5).

Let us finally discuss a few important points with respect to experiments. In the vicinity of the Feshbach transition, where the interaction energy becomes strong, the validity of a single-band Hubbard model becomes questionable. However, this effect is significant only in a region of width α/U around $\nu = 0$ and will not change our conclusions for most regions of the phase diagram for narrow resonances. Quantitative predictions of our model have to be supplemented with standard T-matrix renormalization effects near the MI-SF transition. This requires a more thorough analysis of the role of the optical lattice [13] and is beyond the scope of our work. However, we expect the qualitative predictions of the present theory regarding the Mott phases and the MF-SI transitions to be valid. At high lattice filling, molecules are
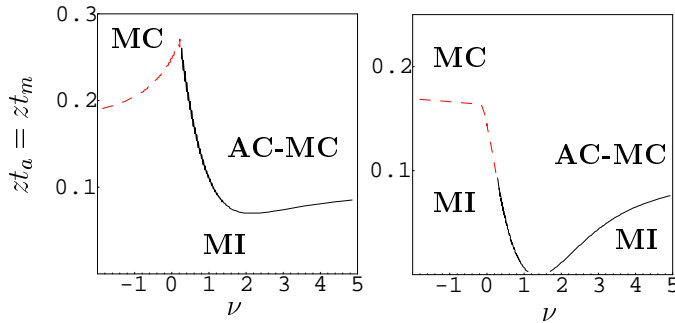

Fig. 5 – Same as Fig. 4 but for $n = 2$. The solid (dashed) lines indicate a transition from a MI to an AC-MC (MC) SF phase.

likely to be unstable due to inelastic three-body collisions; this difficulty does not arise in the $n = 2$ and $n = 1$ Mott phases, which are therefore good experimental candidates to test our predictions. In the presence of the trap potential, superfluid and Mott phases can coexist in certain ranges of experimental parameters, and MI-SF transitions should rather be seen as crossovers than real quantum phase transitions [14]. However, this does not invalidate our main conclusions as stated below (if we understand transitions as crossovers).

In conclusion, we have shown that a Bose gas in an optical lattice near a Feshbach resonance exhibits a very rich phase diagram. Characteristic features of this phase diagram, which are qualitatively robust irrespective of precise numerical parameter values, are: i) MI-SF transitions can be induced either by decreasing the strength of the optical lattice or by varying the magnetic field which controls the detuning from resonance. ii) MI's with odd commensurate density are always unstable to superfluidity on the molecular side of the resonance whatever the strength of the optical lattice potential. iii) MI's with even commensurate density can be stable on both sides of the resonance. iv) For a commensurate density the ground-state may undergo several MI-SF or SF-MI transitions as the magnetic field is varied through the resonance. We therefore expect a measurement of the momentum distribution function [1] to display several transitions between peaked interference patterns (SF state) and featureless uniform distribution (MI) as the magnetic field is varied. Another possible experiment would be to measure the evolution of the excitation spectrum as the magnetic field is varied, using two-photon Bragg spectroscopy [15].

REFERENCES

[1]   M. Greiner, O. Mandel, T. Esslinger, T.W. Hänsch, and I. Bloch, Nature **415**, 39 (2002).
[2]   M.P.A. Fisher *et al.*, Phys. Rev. B **40**, 546 (1989); D. Jaksch *et al.*, Phys. Rev. Lett. **81**, 3108 (1998).
[3]   S. Inouye *et al.*, Nature **392**, 151 (1998); E.A. Donley *et al.*, Nature **417**, 529 (2002).
[4]   For a recent review on Feshbach resonances see R.A. Duine and H.T.C. Stoof, Phys. Rep. **396**, 115 (2004).
[5]   An important point in this derivation is that the size of the molecular bound state is much smaller than the lattice period, so that the molecules can be considered as point-like particles of mass $2m$ (with m the atomic mass).
[6]   Since the molecules are heavier than the atoms, we expect $t_m < t_a$.
[7]   See, for instance, S. Sachdev, *Quantum Phase Transitions* (Cambridge University, Cambridge, England, 1999).
[8]   see, for instance, J.W. Negele and H. Orland, *Quantum Many Particle Systems* (Addison-Wesley, 1988).
[9]   See, for instance, J.C. Tolédano and P. Tolédano, *The Landau Theory of Phase Transitions* (World Scientific, 1987).
[10] L. Radzihovsky *et al.*, Phys. Rev. Lett. **92**, 160402 (2004); M.W.J. Romans *et al.*, Phys. Rev. Lett. **93**, 020405 (2004).
[11] Note that there is no SF phase with an AC and no MC. Because of the coupling between atoms and molecules (α term in Eq. (5)), an AC ($\phi_a \neq 0$) would immediately induce a MC ($\phi_m \neq 0$).
[12] The occurrence of first-order phase transitions was overlooked in Ref. [10] where a free energy similar to that in Eq. (5) was studied. First-order phase transitions have nevertheless been predicted in two-component and spin-1 boson systems: A. Kuklov *et al.*, Phys. Rev. Lett. **92**, 050402 (2004); K.V. Kruititsky *et al.*, Phys. Rev. A **70**, 063610 (2004); T. Kimura *et al.*, cond-mat/0408014.
[13] D.B.M. Dickerscheid, U. Al Khawaja, D. van Oosten, H.T.C. Stoof, cond-mat/0409416.
[14] S. Wessel, F. Alet, M. Troyer, and G. Batrouni, Phys. Rev. A **70**, 053615 (2004).
[15] M. Köhl, H. Moritz, T. Stöferle, C. Schori, and T. Esslinger, cond-mat/0404338.